ACS OMEGA

http://pubs.acs.org/journal/acsodf Article

An Extreme Energy-Saving Carbohydrazide Oxidization Reaction Directly Driven by Commercial Graphite Paper in Alkali and Near-Neutral Seawater Electrolytes

Yanqing Wang,* Gaoyuan Li, Han Yan, Shuyan Chen, and Liping Ding*

Cite This: *ACS Omega* 2021, 6, 15737−15741 Read Online

ABSTRACT: The energy-saving anode with low oxidization potential has been an intriguing pursue for earth-abundant seawater electrolysis. In this paper, we first introduced a superior energy-saving carbohydrazide oxidization reaction catalysis system in the anode section, which can be driven by commercial graphite paper with good durability. Combining this catalysis reaction and common graphite paper, the lowest anodic potentials 0.63 V (vs RHE) and 1.09 V (vs RHE) were obtained for driving a 10 mA/cm^2 current density in alkali and near-neutral seawater electrolytes, respectively, outperforming all the as-reported alkali or near-neutral seawater catalysts accordingly to the best of our knowledge.

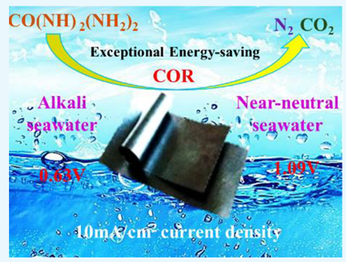

1. INTRODUCTION

Hydrogen as one kind of green energy is gaining more and more attention. Scientists usually employ water electrolysis to generate hydrogen.[1] The water electrolysis process contains hydrogen evolution reaction (HER)[2,3] and oxygen evolution reaction (OER) processes.[4−7] The OER process refers to multielectron transfer and is dynamically sluggish compared with the HER process.[8,9] Initially, noble metal-based catalysts are used to drive the OER process. However, researchers begin to develop earth-abundant catalysts owing to the scarcity of noble metals.[10,11] The as-reported earth-abundant OER catalysts mainly contain compounds that are Ni-based,[12−14] Fe-based,[15] Co-based,[16,17] Cu-based,[18] Mn-based,[19,20] bimetal-based,[21−24] trimetal-based,[25] etc. Although many advanced catalysts have been fabricated, low-cost water electrolysis technology is still highly desired.

To realize more economic water electrolysis, scientists attempt to employ earth-abundant and low-cost seawater electrolysis to replace pure water electrolysis. The seawater electrolysis includes alkali seawater electrolysis and neutral or near-neutral seawater electrolysis. Similarly, the anodic potential consumption dominates the main section during the seawater electrolysis, so researchers pay more attention to the fabrication of highly efficient OER catalysts in the anode section. There exists an oxygen evolution reaction and chloride ion oxidation side reaction for the anode section during seawater electrolysis. The selectivity of the OER process will affect the voltage consumption of the electrolysis process. High-performance OER catalysts always have much higher OER selectivity. Alkali conditions are beneficial for oxygen evolution. Herein, scientists first design some noble catalysts, such as RuO_2,[26] $Pb_2Ru_2O_{7-x}$, and so on. To improve the OER selectivity and catalysis performance, many superior earth-abundant catalysts have been prepared, such as Ni-Fe-LDH,[27] NCFPO/C@CC,[28] NiMoN@NiFeN,[29] S-(Ni,Fe)OOH,[30] and so on. Meanwhile, some researchers also study near-neutral seawater electrolysis and fabricate a lot of OER catalysts, such as $Pb_2Ru_2O_{7-x}$, Co-Fe LDH,[31] NiFe LDH,[32] Co-P-B/rGO,[33] and so on. Although scientists have made many works, the anodic potentials of catalysts are still more than 1.40 V (vs RHE) and 1.70 V (vs RHE) for driving a 10 mA/cm^2 current density in alkali and near-neutral seawater electrolytes till now to the best of our knowledge, respectively. Herein, the high anodic potential of catalysts is still the big obstacle for improving seawater electrolysis performance. As such, to solve this problem, the development of a novel energy-saving oxidization reaction catalysis system in the anode section will be highly desired.

2. RESULTS AND DISCUSSION

2.1. Introduction of an Energy-Saving Anodic COR Catalysis System. In this work, we proposed an exceptional energy-saving carbohydrazide oxidization reaction (COR) catalysis system in the anode section for the first time. As shown in Figure 1a, the carbohydrazide molecule contains abundant N−H bonds with reduction properties, which indicates that the carbohydrazide molecule is more easily oxidized. The literature[34] shows that the theoretical oxidized potential of the carbohydrazide molecule is −1.25 V (vs

Received: February 24, 2021
Accepted: May 28, 2021
Published: June 13, 2021

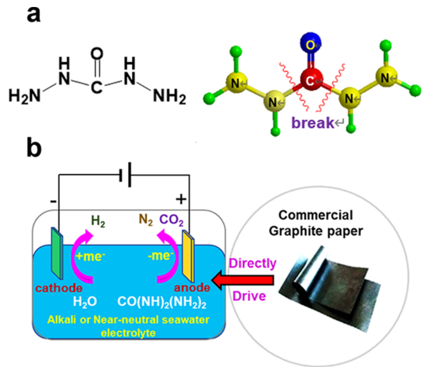

Figure 1. Scheme of an exceptional energy-saving carbohydrazide oxidization reaction catalysis system in alkali or near-neutral seawater electrolytes directly driven by graphite paper. (a) Structural model of the carbohydrazide molecule. (b) Design of the energy-saving carbohydrazide oxidization reaction seawater electrolysis cell.

RHE).[34] The literature[35] demonstrates that a C atom may present a positive charge, a N atom may present a negative charge, and C−N bonds will possibly crack under the catalysis of catalysts for the carbohydrazide molecule similar to the urea molecule.[35] This energy-saving carbohydrazide catalysis system contains carbohydrazide-containing electrolytes and a graphite paper catalytic electrode. As we know, Cl^- corrosion is a potential threat to metal-based catalysts for seawater electrolysis. Carbon materials are more resistant to corrosion than metal materials. Graphite paper as a typical carbon material representative is usually widely used as the conductive electrode. Herein, graphite paper is studied as a catalytic anode in this paper. Combining carbohydrazide-containing electrolytes and a common commercial graphite paper electrode, the lowest anodic oxidization potentials 0.63 V (vs RHE) and 1.09 V (vs RHE) for driving a 10 mA/cm^2 current density were obtained in alkali or near-neutral seawater electrolytes till now, respectively, surpassing all the as-reported alkali or near-neutral seawater electrolysis systems for the anodic reaction section to the best of our knowledge (Tables S1 and S2).

First, the physical property of commercial graphite paper was studied. Figure S1 shows that commercial graphite paper is composed of abundant microscale graphite flakes. As shown in Figure S2, the corresponding matrix carbon element and a small amount of oxygen element were all detected by XPS in the surface of graphite paper. Figure S3 shows that graphite paper presents obvious crystal characterization. PDF #75-2078 shows that the crystal peaks at 26.6 and 54.8° come from the (111) and (222) crystal planes of graphite, respectively.

2.2. COR Catalysis Performance of Graphite Paper in Alkali Seawater Electrolytes. Further, the COR performance of graphite paper in alkali seawater electrolytes was first investigated. As shown in Figure 2a, this graphite paper electrode exhibits good carbohydrazide oxidization reaction catalysis performance in alkali seawater electrolytes, which can drive 10 and 100 mA/cm^2 current densities with demands of 0.63 V (vs RHE) and 1.03 V (vs RHE), respectively. The measured double-layer capacitance (C_{dl}) value of the graphite paper electrode is 24.3 mF/cm^2. According to the calculation method in the Supporting Information, the electrochemical active surface area (ECSA) of the graphite paper electrode is 607.5 cm^2 per 1 cm^2 geometric surface area (GSA) (Figures S4 and S5). The large ECSA value indicates that this electrode has abundant electrochemical active sites.

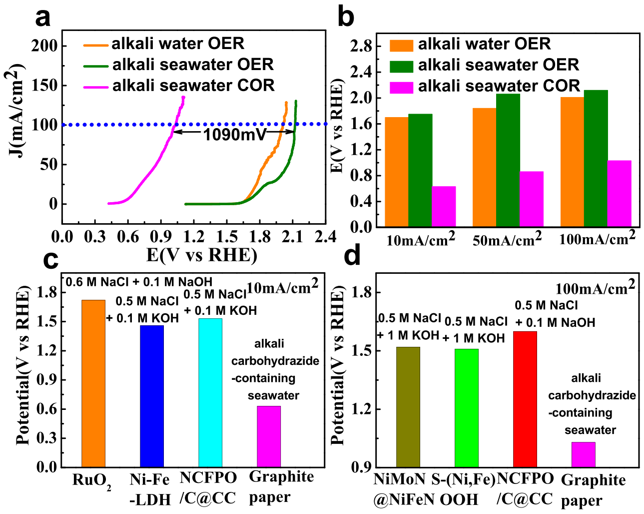

Figure 2. Carbohydrazide oxidization reaction (COR) performance of graphite paper in alkali seawater electrolytes. (a) Comparison of LSV performance of graphite paper for the OER and COR in alkali water and seawater electrolytes. (b) Comparison of potential at 10, 50, and 100 mA/cm^2 current densities of graphite paper for the OER and COR in alkali water and seawater electrolytes. (c) Comparison of the anode oxidization potential between the graphite paper alkali seawater COR catalysis system and other alkali seawater catalysts at a 10 mA/cm^2 current density. (d) Comparison of the anode oxidization potential between the graphite paper alkali seawater COR catalysis system and other alkali seawater catalysts at a 100 mA/cm^2 current density. Note: the involved catalysts in (c) and (d) come from Table S1 in the Supporting Information.

As shown in Figure 2a,b, when the graphite paper drives 10, 50, and 100 mA/cm^2 current densities, the potentials of the carbohydrazide oxidation reaction for the graphite paper electrode are 1120, 1200, and 1090 mV lower than the potential of the seawater oxidation reaction, respectively. Moreover, linear sweep voltammetry (LSV) performance of graphite paper in alkali water and seawater electrolytes is similar. The result indicates that carbohydrazide oxidization technology shows obvious advantages in the energy-saving hydrogen production area compared with the traditional pure seawater oxidization method.

Notably, this graphite paper electrode can drive 10 and 100 mA/cm^2 current densities with the lowest anodic oxidization potentials 0.63 V (vs RHE) and 1.03 V (vs RHE) in alkali seawater electrolytes with the aid of the carbohydrazide oxidization catalysis reaction till now, respectively, outperforming all the as-reported alkali seawater catalysts accordingly to the best of our knowledge (Figure 2c,d and Table S1). The above obtained results confirm that the graphite paper electrode is superior when driving the carbohydrazide oxidization reaction process.

2.3. COR Catalysis Performance of Graphite Paper in Near-Neutral Seawater Electrolytes. Furthermore, the COR performance of graphite paper in near-neutral seawater electrolytes was studied for the first time. As shown in Figure 3a, this graphite paper electrode also presents excellent carbohydrazide oxidization reaction catalysis performance in near-neutral seawater electrolytes, which can drive 5 and 10 mA/cm^2 current densities with demands of 0.96 V (vs RHE) and 1.09 V (vs RHE), respectively. The measured C_{dl} value of the graphite paper electrode is 3.82 mF/cm^2. According to the calculation method in the Supporting Information, the ECSA

https://doi.org/10.1021/acsomega.1c01010
ACS Omega 2021, 6, 15737−15741

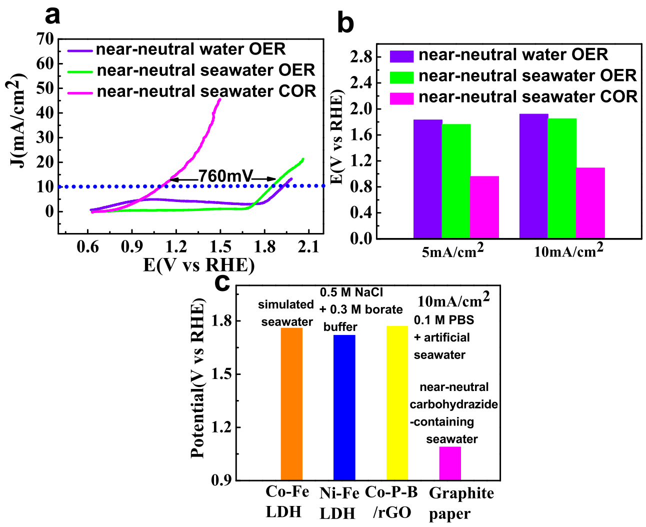

Figure 3. Carbohydrazide oxidization reaction (COR) performance of graphite paper in near-neutral seawater electrolytes. (a) Comparison of LSV performance of graphite paper for the OER and COR in near-neutral water and seawater electrolytes. (b) Comparison of potential at 5 and 10 mA/cm^2 current densities of graphite paper for the OER and COR in neutral water and seawater electrolytes. (c) Comparison of the anode oxidization potential between the graphite paper near-neutral seawater COR catalysis system and other near-neutral seawater catalysts at a 10 mA/cm^2 current density. Note: the involved catalysts in (c) come from Table S2 in the Supporting Information.

of the graphite paper electrode is 95.5 cm^2 per 1 cm^2 GSA (Figures S6 and S7). The large ECSA value demonstrates that this electrode has enriched electrochemical active sites.

As shown in Figure 3a,b, when the graphite paper drives 5 and 10 mA/cm^2 current densities, the potentials of the carbohydrazide oxidation reaction for the graphite paper electrode are 800 and 760 mV lower than the potential of the seawater oxidation reaction in near-neutral seawater electrolytes, respectively. Moreover, the LSV performance of graphite paper in near-neutral water and seawater electrolytes is similar. The above result shows that this carbohydrazide oxidization method shows significant advantages in the energy-saving hydrogen production area compared with the traditional pure near-neutral seawater oxidization method. Importantly, this graphite paper electrode can drive a 10 mA/cm^2 current density with the lowest anodic oxidization potential 1.09 V (vs RHE) in near-neutral seawater electrolytes by using the carbohydrazide oxidization catalysis reaction till now, outperforming all the as-reported near-neutral seawater catalysts to the best of our knowledge (Figure 3c and Table S2). The above obtained results also demonstrate that the graphite paper electrode is excellent for driving the carbohydrazide oxidization reaction process in near-neutral seawater electrolytes.

2.4. COR Catalysis Durability of Graphite Paper in Alkali or Near-Neutral Seawater Electrolytes. Electrochemical durability is also a key issue for COR catalysts in alkali or near-neutral seawater electrolytes. Figure 4a shows that the graphite paper can durably drive a 10 mA/cm^2 current density carbohydrazide oxidation process for at least 10 h in alkali seawater electrolytes. In addition, as shown in Figure 4b, the graphite paper can also stably drive the 10 mA/cm^2 current density carbohydrazide oxidation process for at least 10 h in

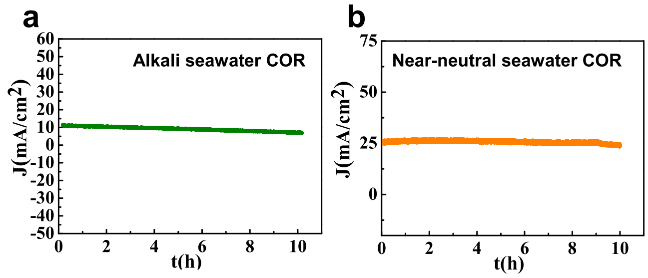

Figure 4. COR durability of graphite paper in alkali or near-neutral seawater electrolytes. (a) Chronoamperometric measurements of the carbohydrazide oxidation reaction at a 10 mA/cm^2 current density for graphite paper in alkali seawater electrolytes. (b) Chronoamperometric measurements of the carbohydrazide oxidation reaction at a 25 mA/cm^2 current density for graphite paper in near-neutral seawater electrolytes.

near-neutral seawater electrolytes. The above results confirm that the common commercial graphite paper is stable for driving the carbohydrazide oxidization reaction process whether in alkali seawater electrolytes or near-neutral seawater electrolytes.

3. CONCLUSIONS

In summary, an exceptional energy-saving carbohydrazide oxidization reaction catalysis system in the anode section was introduced for the first time. Combining common commercial graphite paper and carbohydrazide-containing seawater electrolytes, the lowest anodic oxidization potentials 0.63 V (vs RHE) and 1.09 V (vs RHE) were obtained for driving a 10 mA/cm^2 current density in alkali or near-neutral seawater electrolytes till now, respectively, surpassing all the as-reported alkali or near-neutral seawater catalysts accordingly to the best of our knowledge. This carbohydrazide oxidization reaction catalysis system exhibits good commercial application potential for seawater electrolysis in the energy-saving hydrogen production area.

4. EXPERIMENTAL SECTION

4.1. Materials and Reagents. Highly conductive graphite paper (GP) support was purchased from Latech Scientific Supply Pte. Ltd. Ethyl alcohol, KOH, $Na_2B_4O_7{\cdot}10H_2O$, and carbohydrazide were bought from Sigma-Aldrich Chemical Reagent Co.

4.2. Pretreatment of the Graphite Paper Support. To remove the oil on the surface of GP, a piece of GP was immersed in ethyl alcohol at room temperature for 5 min.

4.3. Physical Characterizations. The surface microstructures of different samples were observed using a ZEISS SEM Supra 40 (attached EDS from Oxford Instrument). XRD patterns of varied samples were determined by a Bruker D8 Advanced Diffractometer System. X-ray photoelectron spectroscopy (XPS, Kratos AXIS Ultra DLD) was employed to investigate the elemental analysis of the surface layer of the samples.

4.4. Electrochemical Measurements. We use the typical three-electrode cell connected to a Corrtest CS2350H electrochemical workstation to investigate the COR process. In this cell, the GP, Hg/HgO, and Pt were used as the working electrode (1 × 1 cm^2), the reference electrode, and the counter electrode, respectively. According to refs 26 and 29, the alkali or near-neutral seawater electrolytes can be artificially

https://doi.org/10.1021/acsomega.1c01010
ACS Omega 2021, 6, 15737−15741

simulated by adding 0.6 M NaCl to 1 M KOH or 0.1 M sodium tetraborate, respectively. Herein, the alkali carbohydrazide-containing seawater electrolyte solution was prepared by adding 0.5 M carbohydrazide into alkali seawater electrolytes and the pH value of the electrolyte is about 14. Similarly, the near-neutral carbohydrazide-containing seawater electrolyte solution was synthesized by adding 0.5 M carbohydrazide into near-neutral seawater electrolytes and the pH value of the electrolyte is about 9. According to the equation $E(\text{RHE}) = E_{\text{Hg/HgO}} + 0.059\text{pH} + 0.098$ V, all the recorded potential values were converted according to the reversible hydrogen electrode (RHE) standard. LSV curves were also recorded with a scan rate of 1 mV/s. Notably, all the electrochemical data in this paper were shown after 100% IR compensation.

■ ASSOCIATED CONTENT

Supporting Information

The Supporting Information is available free of charge at https://pubs.acs.org/doi/10.1021/acsomega.1c01010.

SEM, XPS, XRD, CV, ECSA, and the comparison of anode oxidization potential (PDF)

■ AUTHOR INFORMATION

Corresponding Authors

Yanqing Wang − *School of Chemistry and Chemical Engineering, Nantong University, Nantong 226007, China*; orcid.org/0000-0002-9898-548X; Email: ccewyq@ntu.edu.cn

Liping Ding − *School of Chemistry and Chemical Engineering, Nantong University, Nantong 226007, China*; Email: dingliping@ntu.edu.cn

Authors

Gaoyuan Li − *School of Chemistry and Chemical Engineering, Nantong University, Nantong 226007, China*

Han Yan − *School of Chemistry and Chemical Engineering, Nantong University, Nantong 226007, China*; orcid.org/0000-0003-0868-6230

Shuyan Chen − *School of Chemistry and Chemical Engineering, Nantong University, Nantong 226007, China*

Complete contact information is available at: https://pubs.acs.org/10.1021/acsomega.1c01010

Notes

The authors declare no competing financial interest.

■ ACKNOWLEDGMENTS

The authors thank the National Natural Science Foundation of China (52001173), Natural Science Foundation of Jiangsu Province (BK20200970), General Project of Natural Science Research in Jiangsu Colleges and Universities (20KJB530011), Research Fund of Nantong University (03083054), and Large Instruments Open Foundation of Nantong University (KFJN2038 and KFJN2028) for financial support.

■ REFERENCES

(1) Zhou, H.; Yu, F.; Sun, J.; He, R.; Chen, S.; Chu, C.-W.; Ren, Z. Highly Active Catalyst Derived from A 3D Foam of $Fe(PO_3)_2/Ni_2P$ for Extremely Efficient Water Oxidation. *Proc. Natl. Acad. Sci.* **2017**, *114*, 5607−5611.

(2) Wang, J.; Wei, X.; Song, W.; Shi, X.; Wang, X.; Zhong, W.; Wang, M.; Ju, J.; Tang, Y. Plasmonic Enhancement in Water Splitting Performance for NiFe Layered Double Hydroxide-N_{10}TC MXene Heterojunction. *ChemSusChem* **2021**, *14*, 1948−1954.

(3) Zhang, J.; Liu, Y.; Sun, C.; Xi, P.; Peng, S.; Gao, D.; Xue, D. Accelerated Hydrogen Evolution Reaction in CoS_2 by Transition-Metal Doping. *ACS Energy Lett.* **2018**, *3*, 779−786.

(4) Cheng, X.; Pan, Z.; Lei, C.; Jin, Y.; Yang, B.; Li, Z.; Zhang, X.; Lei, L.; Yuan, C.; Hou, Y. A Strongly Coupled 3D Ternary Fe_2O_3@$Ni_2P/Ni(PO_3)_2$ Hybrid for Enhanced Electrocatalytic Oxygen Evolution at Ultra-High Current Densities. *J. Mater. Chem. A* **2019**, *7*, 965−971.

(5) Zhang, J.; Hu, Y.; Liu, D.; Yu, Y.; Zhang, B. Enhancing Oxygen Evolution Reaction at High Current Densities on Amorphous-Like Ni-Fe-S Ultrathin Nanosheets via Oxygen Incorporation and Electrochemical Tuning. *Adv. Sci.* **2017**, *4*, 1600343.

(6) Wang, M.; Zhang, M.; Song, W.; Zhong, W.; Wang, X.; Wang, J.; Sun, T.; Tang, Y. A Highly Stable $CoMo_2S_4/Ni_3S_2$ Heterojunction Electrocatalyst for Efficient Hydrogen Evolution. *Chem. Commun.* **2021**, *57*, 785−788.

(7) Zhou, H.; Yu, F.; Zhu, Q.; Sun, J.; Qin, F.; Yu, L.; Bao, J.; Yu, Y.; Chen, S.; Ren, Z. Water Splitting by Electrolysis at High Current Densities under 1.6 Volts. *Energy Environ. Sci.* **2018**, *11*, 2858−2864.

(8) Zou, X.; Liu, Y.; Li, G.-D.; Wu, Y.; Liu, D.; Li, W.; Li, H.-W.; Wang, D.; Zhang, Y.; Zou, X. Ultrafast Formation of Amorphous Bimetallic Hydroxide Films on 3D Conductive Sulfide Nanoarrays for Large-Current-Density Oxygen Evolution Electrocatalysis. *Adv. Mater.* **2017**, *29*, 1700404.

(9) Cao, L.-M.; Hu, Y.-W.; Tang, S.-F.; Iljin, A.; Wang, J.-W.; Zhang, Z.-M.; Lu, T.-B. Fe-CoP Electrocatalyst Derived from a Bimetallic Prussian Blue Analogue for Large-Current-Density Oxygen Evolution and Overall Water Splitting. *Adv. Sci.* **2018**, *5*, 1800949.

(10) Zhang, X.; Li, J.; Yang, Y.; Zhang, S.; Zhu, H.; Zhu, X.; Xing, H.; Zhang, Y.; Huang, B.; Guo, S.; Wang, E. $Co_3O_4/Fe_{0.33}Co_{0.66}P$ Interface Nanowire for Enhancing Water Oxidation Catalysis at High Current Density. *Adv. Mater.* **2018**, *30*, 1803551.

(11) Wang, J.; Wei, X.; Wang, X.; Song, W.; Zhong, W.; Wang, M.; Ju, J.; Tang, Y. Plasmonic Au Nanoparticle@$Ti_3C_2T_x$ Heterostructures for Improved Oxygen Evolution Performance. *Inorg. Chem.* **2021**, *60*, 5890−5897.

(12) Chen, L.; Chang, J.; Zhang, Y.; Gao, Z.; Wu, D.; Xu, F.; Guo, Y.; Jiang, K. Fluorine Anion-Enriched Nickel Hydroxyl Oxide as An Efficient Oxygen Evolution Reaction Electrocatalyst. *Chem. Commun.* **2019**, *55*, 3406−3409.

(13) Jiang, W.-J.; Niu, S.; Tang, T.; Zhang, Q.-H.; Liu, X.-Z.; Zhang, Y.; Chen, Y.-Y.; Li, J.-H.; Gu, L.; Wan, L.-J.; Hu, J.-S. Crystallinity-Modulated Electrocatalytic Activity of a Nickel(II) Borate Thin Layer on Ni_3B for Efficient Water Oxidation. *Angew. Chem., Int. Ed.* **2017**, *56*, 6572−6577.

(14) Xia, B.; Wang, T.; Jiang, X.; Li, J.; Zhang, T.; Xi, P.; Gao, D.; Xue, D. N^+-Ion Irradiation Engineering towards the Efficient Oxygen Evolution Reaction on NiO Nanosheet Arrays. *J. Mater. Chem. A* **2019**, *7*, 4729−4733.

(15) Zhang, W.-D.; Yan, X.; Li, T.; Liu, Y.; Fu, Q.-T.; Gu, Z.-G. Metal-Organic Layer Derived Metal Hydroxide Nanosheets for Highly Efficient Oxygen Evolution. *Chem. Commun.* **2019**, *55*, 5467−5470.

(16) Jiang, N.; You, B.; Sheng, M.; Sun, Y. Electrodeposited Cobalt-Phosphorous-Derived Films as Competent Bifunctional Catalysts for Overall Water Splitting. *Angew. Chem., Int. Ed.* **2015**, *54*, 6251−6254.

(17) Ma, T. Y.; Dai, S.; Jaroniec, M.; Qiao, S. Z. Metal-Organic Framework Derived Hybrid Co_3O_4-Carbon Porous Nanowire Arrays as Reversible Oxygen Evolution Electrodes. *J. Am. Chem. Soc.* **2014**, *136*, 13925−13931.

(18) Barnett, S. M.; Goldberg, K. I.; Mayer, J. M. A Soluble Copper-Bipyridine Water-Oxidation Electrocatalyst. *Nat. Chem.* **2012**, *4*, 498−502.

(19) Maayan, G.; Gluz, N.; Christou, G. A Bioinspired Soluble Manganese Cluster as A Water Oxidation Electrocatalyst with Low Overpotential. *Nat. Catal.* **2018**, *1*, 48−54.

(20) Zhao, Y.; Chang, C.; Teng, F.; Zhao, Y.; Chen, G.; Shi, R.; Waterhouse, G. I. N.; Huang, W.; Zhang, T. Defect-Engineered Ultrathin δ-MnO_2 Nanosheet Arrays as Bifunctional Electrodes for Efficient Overall Water Splitting. *Adv. Energy Mater.* **2017**, *7*, 1700005.
(21) Zhou, L.; Guo, M.; Li, Y.; Gu, Q.; Zhang, W.; Li, C.; Xie, F.; Lin, D.; Zheng, Q. One-Step Synthesis of Wire-In-Plate Nanostructured Materials Made of CoFe-LDH Nanoplates Coupled with $Co(OH)_2$ Nanowires Grown on A Ni Foam for A High-Efficiency Oxygen Evolution reaction. *Chem. Commun.* **2019**, *55*, 4218−4221.
(22) Jia, X.; Wu, J.; Lu, K.; Li, Y.; Qiao, X.; Kaelin, J.; Lu, S.; Cheng, Y.; Wu, X.; Qin, W. Organic−Inorganic Hybrids of Fe−Co Polyphenolic Network Wrapped Fe_3O_4 Nanocatalysts for Significantly Enhanced Oxygen Evolution. *J. Mater. Chem. A* **2019**, *7*, 14302−14308.
(23) Chen, G.; Zhou, W.; Guan, D.; Sunarso, J.; Zhu, Y.; Hu, X.; Zhang, W.; Shao, Z. Two Orders of Magnitude Enhancement in Oxygen Evolution Reactivity on Amorphous $Ba_{0.5}Sr_{0.5}Co_{0.8}Fe_{0.2}O_{3-\delta}$ Nanofilms with Tunable Oxidation State. *Sci. Adv.* **2017**, *3*, e1603206.
(24) Zhang, J.; Bai, X.; Wang, T.; Xiao, W.; Xi, P.; Wang, J.; Gao, D.; Wang, J. Bimetallic Nickel Cobalt Sulfide as Efficient Electrocatalyst for Zn-Air Battery and Water Splitting. *Nano-Micro Lett.* **2019**, *11*, 2.
(25) Zhang, B.; Zheng, X.; Voznyy, O.; Comin, R.; Bajdich, M.; García-Melchor, M.; Han, L.; Xu, J.; Liu, M.; Zheng, L.; de Arquer, F. P. G.; Dinh, C. T.; Fan, F.; Yuan, M.; Yassitepe, E.; Chen, N.; Regier, T.; Liu, P.; Li, Y.; Luna, P. D.; Janmohamed, A.; Xin, H. L.; Yang, H.; Vojvodic, A.; Sargent, E. H. Homogeneously Dispersed Multimetal Oxygen-Evolving Catalysts. *Science* **2016**, *352*, 333−337.
(26) Gayen, P.; Saha, S.; Ramani, V. Selective Seawater Splitting Using Pyrochlore Electrocatalyst. *ACS Appl. Energy Mater.* **2020**, *3*, 3978−3983.
(27) Dresp, S.; Dionigi, F.; Loos, S.; de Araujo, J. F.; Spöri, C.; Gliech, M.; Dau, H.; Strasser, P. Direct Electrolytic Splitting of Seawater: Activity, Selectivity, Degradation, and Recovery Studied from the Molecular Catalyst Structure to the Electrolyzer Cell Level. *Adv. Energy Mater.* **2018**, *8*, 1800338.
(28) Song, H. J.; Yoon, H.; Ju, B.; Lee, D.-Y.; Kim, D.-W. Electrocatalytic Selective Oxygen Evolution of Carbon-Coated $Na_2Co_{1-x}Fe_xP_2O_7$ Nanoparticles for Alkaline Seawater Electrolysis. *ACS Catal.* **2020**, *10*, 702−709.
(29) Yu, L.; Zhu, Q.; Song, S.; McElhenny, B.; Wang, D.; Wu, C.; Qin, Z.; Bao, J.; Yu, Y.; Chen, S.; Ren, Z. Non-Noble Metal-Nitride Based Electrocatalysts for High-Performance Alkaline Seawater Electrolysis. *Nat. Commun.* **2019**, *10*, 5106.
(30) Yu, L.; Wu, L.; McElhenny, B.; Song, S.; Luo, D.; Zhang, F.; Yu, Y.; Chen, S.; Ren, Z. Ultrafast Room-Temperature Synthesis of Porous S-Doped Ni/Fe (Oxy)Hydroxide Electrodes for Oxygen Evolution Catalysis in Seawater Splitting. *Energy Environ. Sci.* **2020**, *13*, 3439−3446.
(31) Cheng, F.; Feng, X.; Chen, X.; Lin, W.; Rong, J.; Yang, W. Synergistic Action of Co-Fe Layered Double Hydroxide Electrocatalyst and Multiple Ions of Sea Salt for Efficient Seawater Oxidation at Near-Neutral pH. *Electrochim. Acta* **2017**, *251*, 336−343.
(32) Dionigi, F.; Reier, T.; Pawolek, Z.; Gliech, M.; Strasser, P. Design Criteria, Operating Conditions, and Nickel−Iron Hydroxide Catalyst Materials for Selective Seawater Electrolysis. *ChemSusChem* **2016**, *9*, 962−972.
(33) Li, P.; Jin, Z.; Xiao, D. A One-Step Synthesis of Co−P−B/rGO at Room Temperature with Synergistically Enhanced Electrocatalytic Activity in Neutral Solution. *J. Mater. Chem. A* **2014**, *2*, 18420−18427.
(34) Qi, J.; Benipal, N.; Wang, H.; Chadderdon, D. J.; Jiang, Y.; Wei, W.; Hu, Y. H.; Li, W. Metal-Catalyst-Free Carbohydrazide Fuel Cells with Three-Dimensional Graphene Anodes. *ChemSusChem* **2015**, *8*, 1147−1150.
(35) Li, C.; Liu, Y.; Zhuo, Z.; Ju, H.; Li, D.; Guo, Y.; Wu, X.; Li, H.; Zhai, T. Local Charge Distribution Engineered by Schottky Heterojunctions toward Urea Electrolysis. *Adv. Energy Mater.* **2018**, *8*, 1801775.

https://doi.org/10.1021/acsomega.1c01010
ACS Omega 2021, 6, 15737−15741